Electron-impact study of the NH radical using the *R*-matrix method

Jasmeet Singh Rajvanshi* and K. L. Baluja†
Department of Physics and Astrophysics, University of Delhi, Delhi 110007, India
(Received 19 October 2010; published 16 December 2010)

We have employed the *R*-matrix method to compute elastic (integrated and differential), momentum-transfer, excitation, and ionization cross sections for electron impact on the NH radical. The target states are represented by including correlations via a configuration interaction technique. The results of the static exchange, correlated one-state configuration interaction, and 19-state close-coupling approximation are presented. We have detected a stable anionic bound state $^2\Pi$ of NH^- having the configuration $1\sigma^2 2\sigma^2 3\sigma^2 1\pi^3$. The data of the momentum-transfer cross section, generated from the differential cross section, is used to compute effective collision frequencies over a wide electron temperature range (200–30 000 K). The ionization cross sections are calculated in the binary-encounter Bethe model in which Hartree-Fock molecular orbitals at self-consistent levels are used to calculate kinetic and binding energies of the occupied molecular orbitals. We have included up to the *g* partial wave ($l = 4$) in the scattering calculations. For this dipolar molecule we have used a Born-closure top-up procedure to account for the higher partial waves for the convergence of the cross section.

DOI: 10.1103/PhysRevA.82.062710 PACS number(s): 34.80.Bm, 34.80.Gs, 34.80.Ht

I. INTRODUCTION

The NH radical, also known as the imidogen radical, is an important species in molecular astrophysics [1] and in the study of comets [2]. Several lines of $1\rightarrow 0$ and $2\rightarrow 1$ fundamental vibration-rotation bands of the NH radical were identified in a high-resolution spectrum of supergiant α Orionis by Lambert and Beer [3]. The NH free radical is an important reaction intermediate in some flames, rocket-engine plasmas, electric discharge, and astronomical emission sources [4]. In combustion chemistry, the scientific community has shown a great interest in determining the bond energies and the enthalpies of formation of NH in the study of the combustion of nitramine propellants in aeronautic applications [5]. The Hartree-Fock ground-state configuration of NH is $1\sigma^2 2\sigma^2 3\sigma^2 1\pi^2$, which leads to three low-lying electronic states $X\,^3\Sigma^-$, $a\,^1\Delta$, and $b\,^1\Sigma^+$. The next set of excited states $A\,^3\Pi$ and $c\,^1\Pi$ arises from the electronic configuration $\sigma\ \pi^3$. Cade and Huo have carried out an exhaustive study of the potential energy and spectroscopic constants for the second-row hydrides using the Hartree-Fock-Roothaan wave function [6]. A configuration interaction calculation of the energies of $X\,^3\Sigma^-$, $a\,^1\Delta$, and $b\,^1\Sigma^+$ states of NH has been carried out by [7], using Slater-type functions in which single and double excitations were allowed from the Hartree-Fock configuration. Meyer and Rosmus [8] calculated potential energy curves and dipole moment functions for the ground state of NH by using coupled electron pair approximations. Their calculation of the dipole moment at $R_e = 2.0$ a.u. is 0.6152 a.u. Engelking and Lineberger [9] have determined the electron affinity (EA) of NH by using laser photoelectron spectrometry of NH^-. Their EA value for $X\,^3\Sigma^-$ of NH is 0.381 ± 0.014 eV. Hay and Dunning [10] calculated excitation energies and spectroscopic constants for the $X\,^3\Sigma^-$, $a\,^1\Delta$, $b\,^1\Sigma^+$, $A\,^3\Pi$, and $c\,^1\Pi$ states of NH by using polarization configuration interaction wave functions. Rosmus and Meyer [11] have recommended a value of 13.5 eV for the adiabatic ionization energy of NH by employing a coupled electron pair approach (CEPA) wave function. It is well established experimentally that the ground states of most AH^- ions are bound. The CEPA study [12] has established an adiabatic electron affinity of NH as 0.01 eV, as compared to the experimental value of 0.38 eV [13]. Cvejanovic *et al.* [14] measured the radiation lifetimes of the excited states of the NH radical by using the electron-photon delayed coincidence technique. Frenking and Koch [15] have calculated the electron affinity of NH at different many-body perturbation (MP) levels by using different basis sets. Their best value is 0.18 eV. Joshipura *et al.* [16] have obtained the ionization cross section by electron impact on NH through a complex optical potential. The ionization cross section is extracted through the absorption cross section. The energy range considered in their work is 20–2000 eV.

The present study uses the *ab initio* *R*-matrix method to low-energy scattering of the NH molecule in the fixed nuclei approximation. The calculations use the UK molecular *R*-matrix code [19,20]. The *R*-matrix method has the advantage over other scattering methods in providing cross sections at a large number of scattering energies efficiently. It also has the ability to include correlation effects and give an adequate representation of several excited states of the molecule [21]. We are interested in the low-energy region ($\leqslant 10$ eV) which is a natural ground for the *R*-matrix method. The incoming electron can occupy one of the many unoccupied molecular orbitals or it can excite any of the occupied molecular orbitals as it falls into another one. These processes give rise to the phenomenon of resonances forming a negative molecular ion for a finite time before the resonance decays into energetically open channels.

Electron-scattering calculations are performed at the static exchange, one-state configuration interaction (CI), and 19-state close-coupling approximation in which we have retained 19 target states in the *R*-matrix formalism. The integrated elastic, differential, and momentum cross sections for electron

*Also at Keshav Mahavidyalaya, Physics and Electronics Department, University of Delhi; rajvanshi_jasmeet@yahoo.co.in
†kl_baluja@yahoo.com

impact on the NH molecule from its ground state are reported. The excitation cross sections from the ground state to the few low-lying excited states have also been calculated. We have also computed the binary-encounter-Bethe (BEB) ionization cross section [22,23]. The BEB cross sections depend only on the binding energies, kinetic energies, and the occupation number of the occupied molecular orbitals of the target, and on the energy of the incident electron. We have also shown a comparison of the calculated momentum transfer cross section (MTCS) for the NH radical and the PH radical [24]. The PH radical, like its isovalent first-row radical NH, is an open-shell system with an unpaired π^2 ground-state electronic configuration. The momentum-transfer croctions calculated in the *R*-matrix approximation have been used to calculate the effective collision frequency for NH and PH radicals, over a wide electron temperature range (200–30 000 K).

II. METHOD

A. Theory

In an *R*-matrix approach [26,27], the configuration space of the scattering system is divided into two spatial regions: an inner region and an outer region. These regions are treated differently in accordance with the different interactions in each region. The center of the *R*-matrix sphere coincides with the center of mass of the molecule. When the scattering electron leaves the inner region, the other target electrons are confined to the inner region. In the present work the *R*-matrix boundary radius dividing the two regions was chosen to be $10a_0$, centered at the NH center of mass. This sphere encloses the entire charge cloud of the occupied and virtual molecular orbitals included in the calculation. At $10a_0$, the amplitudes of the molecular orbitals are less than $10^{-5}a_0^{-3/2}$. However, the continuum orbitals have finite amplitudes at the boundary. Inside the *R*-matrix sphere, the electron-electron correlation and exchange interactions are strong. Short-range correlation effects are important for the accurate prediction of large-angle elastic scattering, and exchange effects are important for spin-forbidden excitation cross sections. A multicentered CI wave function expansion is used in the inner region. The calculation in the inner region is similar to a bound-state calculation, which involves the solution of an eigenvalue problem for $(N+1)$ electrons in the truncated space, where there are N target electrons and a single scattering electron. Most of the physics of the scattering problem is contained in this $(N+1)$ electron bound-state molecular-structure calculation. Outside the sphere, only long-range multipolar interactions between the scattering electron and the various target states are included. Because only direct potentials are involved in the outer region, a single center approach is used to describe the scattering electron via a set of coupled differential equations. The *R*-matrix is a mathematical entity that connects the two regions. It describes how the scattering electron enters and leaves the inner region. In the outer region, the *R*-matrix on the boundary is propagated outward [28,29] until the inner-region solutions can be matched with asymptotic solutions, thus yielding physical observables such as cross sections. We include only the dipole and quadrupole moments in the outer region.

In the polyatomic implementation of the UK molecular *R*-matrix code [19,20], the continuum molecular orbitals are constructed from atomic Gaussian-type orbitals (GTOs) using basis functions centered on the center of gravity of the molecule. The main advantage of GTOs is that integrals involving them over all space can be evaluated analytically in closed form. However, a tail contribution is subtracted to yield the required integrals in the truncated space defined by the inner region [19].

The target molecular orbital space is divided into core (inactive), valence (active), and virtual orbitals. The target molecular orbitals are supplemented with a set of continuum orbitals, centered on the center of gravity of the molecule. The continuum basis functions used in polyatomic *R*-matrix calculations are Gaussian functions and do not require fixed boundary conditions. First, target and continuum molecular orbitals are orthogonalized using Schmidt orthogonalization. Then symmetric or Löwdin orthogonalization is used to orthogonalize the continuum molecular orbitals among themselves and remove linearly dependent functions [19,30]. In general, and in this work, all calculations are performed within the fixed-nuclei approximation. This is based on the assumption in which electronic, vibrational, and rotational motions are uncoupled.

In the inner region, the wave function of the scattering system, consisting of target plus scattering electrons, is written using the CI expression

$$\Psi_k^{N+1} = A\sum_i \phi_i^N(x_1,\ldots,x_N)\sum_j \xi_j(x_{N+1})a_{ijk} + \sum_m \chi_m(x_1,\ldots,x_N,x_{N+1})\,b_{mk}, \quad (1)$$

where A is an antisymmetrization operator, x_N is the spatial and spin coordinates of the Nth electron, ϕ_i^N represents the ith state of the N-electron target, ξ_j is a continuum orbital spin coupled with the scattering electron, and k refers to a particular *R*-matrix basis function. Coefficients a_{ijk} and b_{mk} are variational parameters determined as a result of the matrix diagonalization. To obtain reliable results, it is important to maintain a balance between the N-electron target representation ϕ_i^N and the $(N+1)$ electron-scattering wave function. The summation in the second term of Eq. (1) runs over configurations χ_m, where all electrons are placed in target-occupied and virtual molecular orbitals. The choice of appropriate χ_m is crucial in this [31]. These are known as L^2 configurations and are needed to account for orthogonality relaxation and for correlation effects arising from virtual excitation to higher electronic states that are excluded in the first expansion. The wave function ψ_k^{N+1} is independent of the scattering energy but is used to construct the energy-dependent *R* matrix on the boundary. The basis for the continuum electron is parametrically dependent on the *R*-matrix radius and provides a good approximation to an equivalent basis of orthonormal spherical Bessel functions [32]. In the one-state CI model, we have included the ground state only, but have used the CI wave function to describe it. In the 19-state model calculation, each target state is represented by a CI wave function since we can include only a finite number of excited states, which implies that the contribution of the target continuum is taken into account. This

TABLE I. Properties of the NH target, ground-state energy, and dipole moment (in a.u.) and the ionization potential (IP, in eV) and rotational constant (B_e, in cm^{-1}), SCF at bond length $R_e = 1.94a_0$, and CI at bond length $R_e = 2.0a_0$. The experimental values, from [6], are given in the square brackets.

	Present work					
	SCF	CI	SCF[a]	CEPA[a]	CI[b]	SPDCI-VR[c]
E	−54.96 754	−55.00 341	−54.97 353	−55.136 763	−54.97 806 [−55.2520]	−55.13 180
μ	0.685	0.659	0.650	0.621	0.642	0.594
IP	14.56	14.56			12.82 [13.1 ± 0.1]	
B_e	17.023	16.007	17.28	16.60	17.319 [16.668]	16.44

[a]Meyer and Rosmus [8].
[b]Cade and Huo [6].
[c]Goldfield and Kirby [18].

limits the effect of polarization interaction in the scattering calculations.

B. NH target model

Diradicals are a species with a pair of degenerate (equal energy) molecular orbitals and two electrons. A diradical can occur in a triplet and in a singlet state. The oxygen we breathe in is a diradical in a triplet state. The ground-state electronic configuration (π^2) of the NH molecule has two unpaired electrons occupying two degenerate molecular orbitals. These orbitals are antibonding and hence NH is paramagnetic. The molecule NH is a linear open-shell system that has ground state $X\,^3\Sigma^-$ in the $C_{\infty v}$ point group, which is reduced to the C_{2v} point group when the symmetry is lowered. In the R-matrix suite of programs, the highest Abelian group is D_{2h} and therefore we work in the C_{2v} point group, which is a subset of the D_{2h} point group. The results are reported in the natural symmetry point group as well as in the C_{2v} point group for the sake of convenience. We used a double zeta plus polarization (DZP) Gaussian basis set [33] contracted as (9,5,1)/(4,2,1) for N and (4,1)/(2,1) for H. We avoided using diffuse functions as these would extend outside the R-matrix box. We first performed an self-consistent field (SCF) calculation for the ground state of the NH molecule with the chosen DZP basis set and obtained an occupied and virtual set of molecular orbitals.

The Hartree-Fock electronic configuration for the ground state is $1\sigma^2 2\sigma^2 3\sigma^2 1\pi^2$, which gives rise to the lowest-lying $X\,^3\Sigma^-$, $a\,^1\Delta$, and $b\,^1\Sigma^+$ states. The energy of the occupied 1π orbital is −14.56 eV and by Koopman's theorem it is the first ionization energy. Since the SCF procedure is inadequate to provide a good representation of the target states, we improve the energy of the ground as well as the excited states by using CI wave functions. This lowers the energies and the correlation introduced provides a better description of the target wave-function and excitation energies. In our limited CI model, we keep two electrons frozen in the $1\sigma^2$ configuration and allow the remaining six electrons to move freely in molecular orbitals 2σ, 3σ, 4σ, 5σ, 1π, and 2π. The CI ground-state energy for the NH molecule is −55.003 410 hartrees, at a bond length of $R_e = 2.0a_0$. We computed the value of vertical electronic affinity (VEA), which is 0.034 eV, by performing a bound-state calculation of NH^- by including the continuum electron basis functions centered at the origin. We detect a stable bound state of NH^- with $^2\Pi$ symmetry having the configuration $1\sigma^2 2\sigma^2 3\sigma^2 1\pi^3$.

To provide additional information on the charge distribution in the NH molecule, we have also calculated the dipole and quadrupole moments. In our CI model the dipole moment and the absolute values of quadrupole component Q_{20} for the ground state are 0.659 and 0.378 a.u., respectively. The values of the ground-state energy, the dipole moment, the ionization potential, and the rotational constant are compared with other work in Table I.

In Table II, we list the vertical excitation energies and the number of configuration state functions (CSFs) for the target

TABLE II. The vertical excitation energies (VEE, in eV) and N, the number of CSFs for the target states of NH at bond length $R_e = 2.0a_0$. The experimental values, from [17], are given in the square brackets.

State $C_{2v}/C_{\infty v}$	Present work (VEE in eV)	Previous work[a] (VEE in eV)	POL-CI[b] (VEE in eV)	CASSCF[c] (VEE in eV)	CASPT2[c] (VEE in eV)	N
$X\,^3A_2/X\,^3\Sigma^-$	0.0					864
$a(^1A_2,^1A_1)/a\,^1\Delta$	1.88	1.6	1.96	1.92	1.616 [1.56]	584 696
$b(^1A_1)/b\,^1\Sigma^+$	2.7	2.67	2.84	2.60	2.656 [2.63]	696
$A\,^3B_1,^3B_2/A\,^3\Pi$	3.8	3.69	4.08	3.86	3.747 [3.70]	858
$c\,^1B_2,^1B_1/c\,^1\Pi$	5.95	5.42	6.06	5.72	5.520 [5.43]	620
$d(^1A_1)/d\,^1\Sigma^+$	10.84	10.32		10.57	10.484 [10.311]	696

[a]Cvejanovic *et al.* [14].
[b]Hay *et al.* [10].
[c]Rajendra *et al.* [17].

TABLE III. Comparison of dipole moments (μ in a.u.) for the target states of NH, at bond length $R_e = 2.0a_0$, with [10].

State	Dipole moment[a] (μ in a.u.)	Dipole moment (this work) (μ in a.u.)
$a\,^1\Delta$	0.6126 ($1.955a_0$)	0.6634
$b\,^1\Sigma^+$	0.5822 ($1.956a_0$)	0.6482
$A\,^3\Pi$	0.5520 ($1.958a_0$)	0.6479
$c\,^1\Pi$	0.7125 ($2.081a_0$)	0.7545

[a]Hay *et al.* [10].

states. The vertical excitation energies are in good agreement with experimental [14] and other theoretical work [10,17]. The singlet-singlet ($^1\Delta$-$^1\Sigma^+$) splitting value of 0.82 eV is in better agreement with the corresponding value of 0.80 eV with the results of [7].

In Table III, we have compared the dipole moments of the excited states $a\,^1\Delta$, $b\,^1\Sigma^+$, $A\,^3\Pi$, and $c\,^1\Pi$ with the work of [10]. These values are given at slightly different bond lengths which are also shown in Table III. The agreement between our results and that of [10] is quite good. We have also compared the transition moments of the allowed transitions $^3\Sigma^- \rightarrow {}^3\Pi$, $^1\Delta \rightarrow {}^1\Pi$, and $^1\Sigma^+ \rightarrow {}^1\Pi$ in Table IV, at a bond length of $R_e = 2.00a_0$. We notice, once again, that the agreement is quite satisfactory. This comparison shows that the use of wave functions of the ground and the excited states employed in the scattering calculations are of good quality.

C. Scattering model

The lowest three states of NH arise from three different asymptotic atomic limits. We impose a chemically reasonable restriction on the 1σ orbital to be doubly occupied. This is nearly the N $1s$ orbital, which remains frozen during the interaction. In the limit of infinite separation the system approaches a ground-state hydrogen atom (^2S) and a nitrogen atom in a $(1s^2 2s^2 2p^3)(^4S)$, (^2D), (^2P) state for the $^3\Sigma^-$, $^1\Delta$, and $^1\Sigma^+$ molecular states, respectively. We have included 19 target states (two of $^1A_2$, four of $^3A_2$, three of $^1A_1$, two of $^3A_1$, two of $^1B_1$, two of $^3B_1$, two of $^1B_2$, and two of $^3B_2$) in the trial wave function describing the electron plus target system. However, excitation cross sections are reported only for the three excited states ($a\,^1\Delta$, $b\,^1\Sigma^+$, and $A\,^3\Pi$). Calculations were performed for doublet and quartet scattering states with A_1, A_2, B_1, and B_2 symmetries. Continuum orbitals up to $l = 4$ (g partial wave) were included in the scattering calculation.

TABLE IV. Comparison of transition moments (in a.u.) of allowed transitions for NH, at bond length $R_e = 2.0a_0$, with [10].

Transition	Transition moment[a] (in a.u.)	Transition moment (this work) (in a.u.)
$^3\Sigma^- \rightarrow {}^3\Pi$	0.2668	0.3226
$^1\Delta \rightarrow {}^1\Pi$	0.1681	0.2097
$^1\Sigma^+ \rightarrow {}^1\Pi$	0.0833	0.0972

[a]Hay *et al.* [10].

TABLE V. NH molecular orbital binding and average kinetic energies for the DZP basis set at equilibrium geometry. $|B|$ is the binding energy (eV), U is the kinetic energy (eV), and N is the occupation number.

Molecular orbital	$\lvert B\rvert$ (eV)	U (eV)	N
1σ ($1a_1$)	424.72	602.33	2
2σ ($2a_1$)	28.41	53.50	2
3σ ($3a_1$)	14.90	42.95	2
1π ($1b_1$)	7.28	49.08	1
1π ($1b_2$)	7.28	49.08	1

Due to the presence of the long-range dipole interaction, the elastic cross sections are formally divergent in the fixed-nuclei approximation as the differential cross section is singular in the forward direction. To obtain converged cross sections, the effect of rotation must be included along with a very large number of partial waves. The effects of partial waves with $l > 4$ were included using a Born correction via a closure approach [34]. Our partial g-wave cross section using the R-matrix method nearly coincided with the g-wave Born results. This establishes the correctness of our procedure to use Born correction beyond the g-partial wave.

III. RESULTS

A. Elastic and inelastic total cross sections

The ground-state electronic configuration of NH has two unpaired π electrons. Due to vacancy in the 1π orbital of the ground state of NH, the scattering electron can occupy it forming a stable anionic ground state of NH with a symmetry $^2\Pi$. In our 19-state model, we found an R-matrix pole at $-55.004\,66$ a.u. at R_e in the scattering symmetry $^2\Pi$ which is lower than the energy $-55.003\,41$ a.u. of ground state $X\,^3\Sigma^-$ of NH, which indicates the detection of an anionic bound state. We calculated the bound-state energies of this anionic $^2\Pi$ state at different bond lengths by performing an L^2-type calculation in which we placed the scattering electron at the center of mass of the molecule.

The retention of a large number of closed electronic excitation channels in a 19-state model provides the necessary polarization potential in an *ab initio* way; this polarization potential is critical in determining the resonance parameters of the detected resonances. In Fig. 1 we have presented the elastic cross sections of the electron impact on the NH molecule at R_e for a 19-state calculation.

In Figs. 2–4 we have shown the inelastic cross sections from the ground state to the three physical states whose vertical excitation thresholds along, and the number of CSFs included in the CI expansion are given in Table II.

In Figs. 2 and 3 we have shown the comparison of the excitation cross sections for $X\,^3\Sigma^-$-$a\,^1\Delta$ transition and $X\,^3\Sigma^-$-$b\,^1\Sigma^+$ transition, respectively, of the NH molecule with PH [24] and O_2 [25]. The cross sections for PH are higher than those of NH since it is a bigger molecule. The cross sections of isovalent O_2 are lower than these due to the fact that it is nonpolar.

Figure 4 depicts the excitation cross section for the optically allowed transition $X\,^3A_2(X\,^3\Sigma^-)$-$A\,^3B_1/^3B_2(A\,^3\Pi)$.

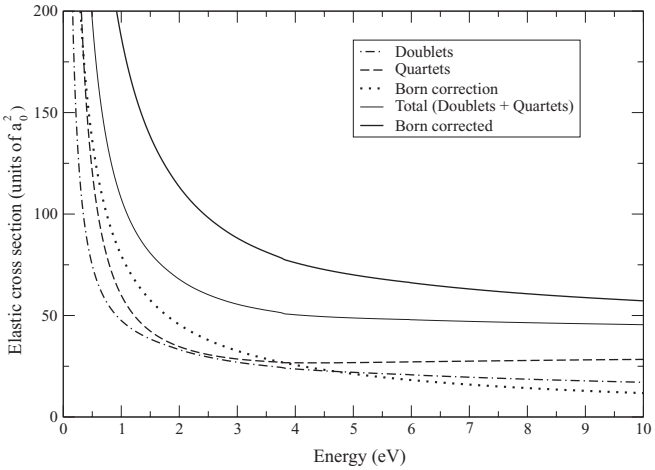

FIG. 1. Elastic cross sections of the electron impact on the NH molecule at R_e for 19-state calculations: dashed dotted curve, doublets sum; dashed curve, quartets sum; thin solid curve, total (doublets + quartets); dotted curve, Born correction; thick solid line, Born corrected (sum of doublets, quartets, and Born correction).

The contribution of quartet and doublet symmetries is shown separately. The contribution of the quartets is once again higher than that of the doublet symmetries. The Born correction is also included for this dipole transition to include the contribution of the higher partial waves that are not included in the R-matrix calculations.

B. Ionization cross section

Figure 5 shows the electron-impact ionization cross section of NH from threshold 14.56 to 5000 eV by using the standard formalism of the binary-encounter-Bethe (BEB) model [22,23]. This formalism requires the binding energy and kinetic energy of each occupied orbital in a molecular structure calculation. The ionization cross section rises from a threshold to a peak value of 2.768 Å^2 at 74.98 eV and then shows $\ln E/E$ behavior as E approaches higher values. We have also shown the results of previous theoretical work [16]. Except at the peak, we have good agreement with this theoretical work. The molecular orbital data used in the calculation of the BEB cross section is given in Table III which is generated at the SCF level. The BEB ionization cross section σ is obtained by summing over each orbital cross section σ_i, where

$$\sigma_i(t) = \frac{s}{t+u+1}\left[\frac{1}{2}\left(1-\frac{1}{t^2}\right)\ln t + \left(1-\frac{1}{t}\right) - \frac{\ln t}{t+1}\right], \tag{2}$$

where $t = T/B$, $u = U/B$, and $s = 4\pi a_0^2 N(R/B)^2$. Here, R is the Rydberg energy, T is the kinetic energy of the incident electron, U is the orbital kinetic energy, N is the electron occupation number, and B is the binding energy of the orbital. The relevant data for U and B is given in Table V.

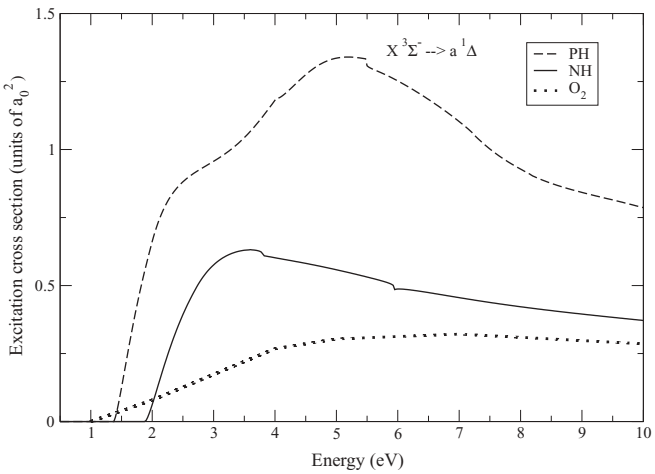

FIG. 2. Comparison of electron-impact excitation cross sections from the ground $X\,^3\Sigma^-$ ($^3A_2$) state to the $a\,^1\Delta/[a(^1A_2/^1A_1)]$ of the NH molecule with PH [24] and O_2 [25].

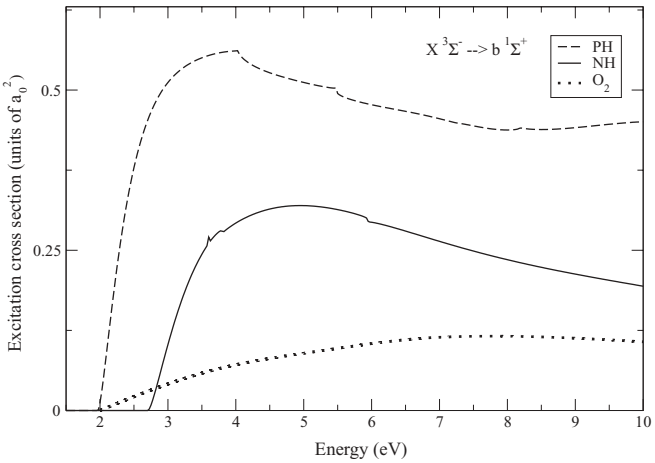

FIG. 3. Comparison of electron-impact excitation cross sections from the ground $X\,^3\Sigma^-$ ($^3A_2$) state to $b\,^1\Sigma^+/[b(^1A_1)]$ of the NH molecule with PH [24] and O_2 [25].

C. Differential cross section

The evaluation of the differential cross sections (DCS) provides a more stringent test for any theoretical model. The

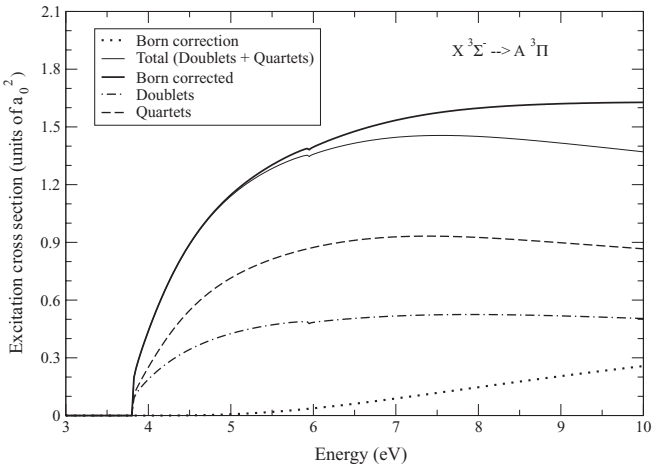

FIG. 4. Electron-impact excitation cross sections from the ground $X\,^3\Sigma^-$ ($^3A_2$) state of the NH molecule to the $A\,^3\Pi$ ($^3B_1/^3B_2$) state for 19-states calculation: dashed dotted curve, doublets sum; dashed curve, quartets sum; thin solid line, total (doublets + quartets); dotted curve, Born correction; thick solid line, Born corrected.

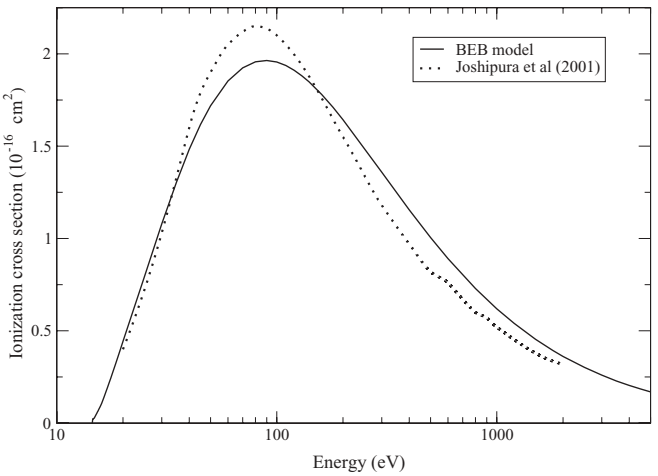

FIG. 5. Electron-impact BEB ionization cross sections of the NH molecule: dotted curve, Joshipura *et al.* [16]; solid line, our BEB model.

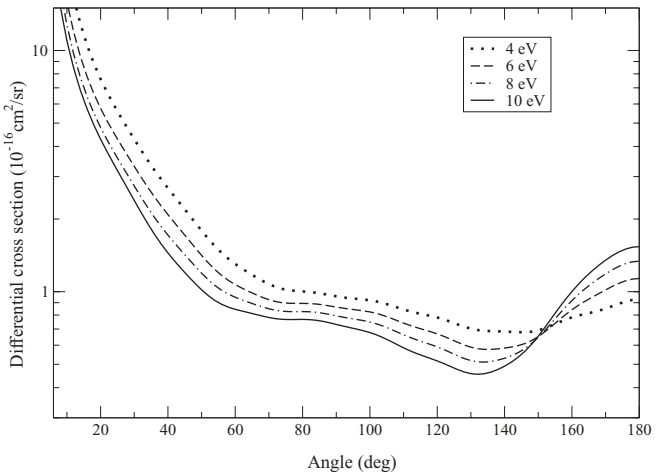

FIG. 6. Differential cross sections at 4, 6, 8, and 10 eV for the one-state CI model (with spin average) at R_e: dotted curve, 4 eV; dashed curve, 6 eV; dashed dotted curve, 8 eV; solid curve, 10 eV.

rotational excitation cross sections for electron impact on a neutral molecule can be calculated from the scattering parameters of elastic scattering in the fixed nuclei approximation provided the nuclei are assumed to be of infinite masses [35]. In particular, starting from an initial rotor state $J = 0$, the sum of all transitions from the $J = 0$ level to a high enough J value for convergence is equivalent to the elastic cross section in the fixed nuclei approach. We have employed this methodology to extract rotationally elastic and rotationally inelastic cross sections from the K-matrix elements calculated in the one-state R-matrix model. The DCS for a general polyatomic molecule is given by the familiar expression

$$\frac{d\sigma}{d\Omega} = \sum_L A_L P_L(\cos\theta), \tag{3}$$

where P_L is a Legendre polynomial of order L. The A_L coefficients have already been discussed in detail [36]. For a polar molecule this expansion over L converges slowly. To circumvent this problem, we use the closure formula

$$\frac{d\sigma}{d\Omega} = \frac{d\sigma^B}{d\Omega} + \sum_L \left(A_L - A_L^B\right) P_L(\cos\theta). \tag{4}$$

The superscript B denotes that the relevant quantity is calculated in the Born approximation with an electron-point dipole interaction. The convergence of the series is now rapid since the contribution from the higher partial waves to the DCS is dominated by the electron-dipole interaction. The quantity $\frac{d\sigma}{d\Omega}$ for any initial rotor state $|Jm\rangle$ is given by the sum over all final rotor states $|J'm'\rangle$,

$$\frac{d\sigma}{d\Omega} = \sum_{J'm'} \frac{d\sigma}{d\Omega}(Jm \to J'm'), \tag{5}$$

where J is the rotational angular momentum and m is its projection on the internuclear axis. To obtain converged results, we calculate the maximum value of $J' = 5$. We have calculated the DCS by using the POLYDCS program of Sanna and Gianturco [37], which requires basic molecular input parameters along with K matrices evaluated in a particular scattering calculation. We have used this code to compute the DCS in a one-state CI model. Since NH is an open-shell molecule having $X\,^3\Sigma^-$ as its ground state, the spin coupling between this target state and the spin of the incoming electron allows two spin-specific channels, namely, the doublet (D) and quartet (Q) couplings. The spin-averaged DCS for elastic electron scattering from the NH radical are calculated by using the statistical weight $2/6$ for doublet and $4/6$ for quartet scattering channels. We then use Eq. (3) as follows to calculate DCS:

$$\frac{d\sigma}{d\Omega} = \frac{1}{3}\left[2\left(\frac{d\sigma}{d\Omega}\right)^Q + \left(\frac{d\sigma}{d\Omega}\right)^D\right], \tag{6}$$

where $(\frac{d\sigma}{d\Omega})^{Q,D}$ represent DCS for the quartet and doublet cases, respectively.

In Fig. 6 we have displayed spin-averaged DCS at 4, 6, 8, and 10 eV in the one-state CI model at R_e. Besides this, the data on the DCS is further used to calculate the MTCS

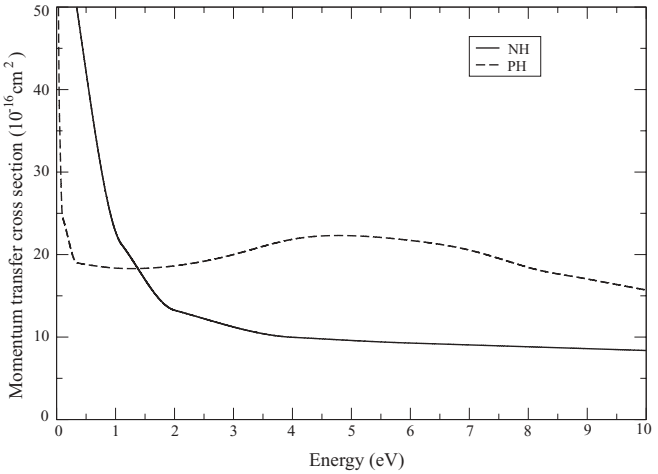

FIG. 7. Momentum-transfer cross sections (MTCS) at different energies of NH and PH [24] radicals, for a one-state CI model: solid curve, NH; dashed curve, PH.

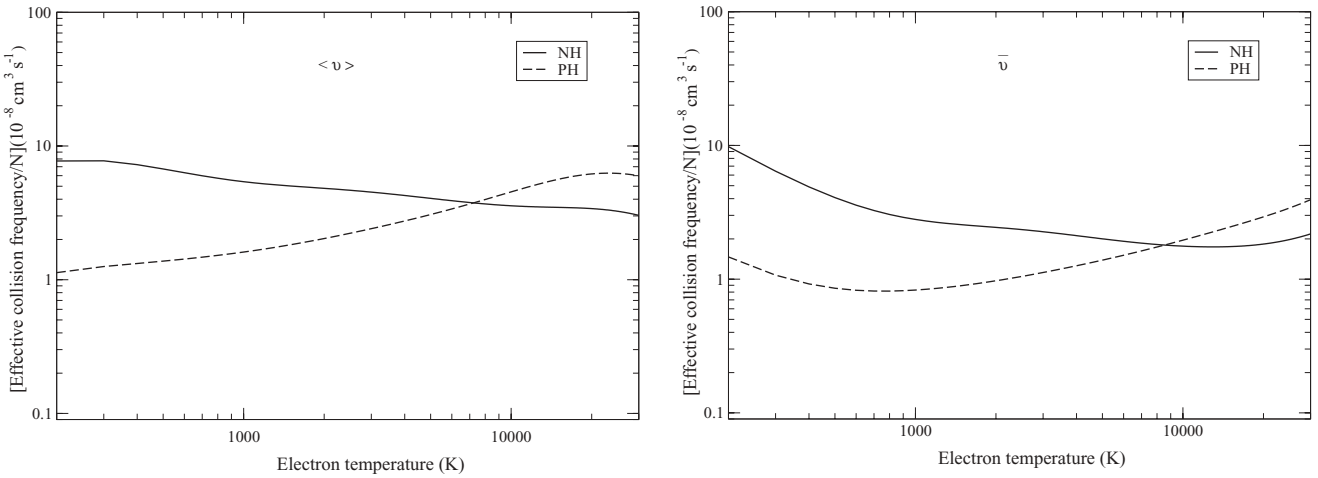

FIG. 8. Comparison of effective collision frequency, as a function of electron temperature, for NH and PH radicals: solid curve, NH; dashed curve, PH.

that shows the importance of backward angle scattering. Since the DCS are not very sensitive to correlation effects for backward scattering, we expect our MTCS to be quite reliable in the 0.02–10 eV range. These are calculated in the one-state CI model with the inclusion of spin averaging. MTCS provide useful input in solving the Boltzmann equation for the electron distribution function. In contrast to the diverging nature of the DCS in the forward direction, the MTCS show no singularity due to the weighting factor $(1-\cos\theta)$, where θ is scattering angle. This factor vanishes as $\theta \to 0$. The MTCS are useful in the study of electrons drifting through a molecular gas. When a swarm of electrons travel through a molecular gas under the influence of an electric field, several transport observables, such as diffusion coefficient D and mobility μ, can be obtained if we have a knowledge of the momentum-transfer cross sections. In Fig. 7, we have shown a comparison of the calculated MTCS for the NH radical, and the PH radical [24]. Beyond 1.5 eV, the MTCS for PH are higher than their corresponding values for the NH radical.

D. Effective collision frequency of electrons

The effective electron-neutral collision frequency $\langle v\rangle$ which is averaged over a Maxwellian distribution can be obtained from the momentum-transfer cross section $Q^{(m)}(v)$ as follows [38]:

$$\langle v\rangle = \frac{8}{3\pi^{1/2}} N\left(\frac{m_e}{2kT_e}\right)^{5/2} \int_0^\infty v^5 Q^{(m)}(v)\exp\left(\frac{-m_e v^2}{2kT_e}\right) dv, \tag{7}$$

where m_e and T_e are the electron mass and electron temperature, respectively, k is Boltzmann's constant, v is the electron velocity, and N is the number density of the gas particles. The averaging is over a Maxwellian speed distribution function for an electron temperature T_e which is given by

$$f(v) = 4\pi v^2 \left(\frac{m_e}{2\pi kT_e}\right)^{3/2} \exp\left(\frac{-m_e v^2}{2kT_e}\right). \tag{8}$$

This type of collision frequency is often used to evaluate the energy transfer between particles. Alternatively, the effective collision frequency for electrons can be defined from the dc conductivity as follows [38,39]:

$$\bar{\nu}^{-1} = \frac{8}{3\pi^{1/2}N}\left(\frac{m_e}{2kT_e}\right)^{5/2} \int_0^\infty \frac{v^3}{Q^{(m)}(v)}\exp\left(\frac{-m_e v^2}{2kT_e}\right) dv. \tag{9}$$

This explicit form of effective collision frequency $\bar{\nu}$ is related to the drift velocity of electrons in a gas, insofar as a Maxwell distribution can be assumed. When $Q^{(m)}(v)$ is proportional to v^{-1}, the two effective collision frequencies $\langle v\rangle$ and $\bar{\nu}$ agree. In Fig. 8, we have shown the comparison of both types of effective collision frequencies for NH and PH radicals, as a function of electron temperature. It is to be noted that $\langle v\rangle$ lies higher than $\bar{\nu}$ in the electron temperature range (200–30 000 K).

IV. CONCLUSIONS

This is a comprehensive *ab initio* study of electron impact on the NH molecule using the UK molecular *R*-matrix codes. Elastic (integrated and differential), momentum-transfer, excitation, and ionization cross sections have been presented. The results of the static-exchange, one-state CI, and 19-state close-coupling approximation are presented. We detect a stable bound state of NH^- having configuration $1\sigma^2 2\sigma^2 3\sigma^2 1\pi^3$. The target states are represented by including correlations via a configuration interaction technique. Our CI model yields a dipole moment of 1.676 Debye at the equilibrium N-H bond length of $2.0a_0$ that agrees with experimental value 1.621 D [17]. The vertical excitation energies are in good agreement with experimental [14] and other theoretical work [10]. The dipole moments of the excited states and the transition moments of allowed transition compare well with the other theoretical work implying the good quality of the wave function employed in the scattering calculation. For the ionization cross section we have performed the standard BEB model [23] and compared our results with other theoretical work [16]. The derived MTCS from the DCS, and two types of effective collision frequencies have also been presented that may be useful to the scientific community.

[1] R. E. Roach, Astrophys. J. **89**, 99 (1939).
[2] P. Swings, C. T. Elvey, and H. W. Babcock, Astrophys. J. **94**, 320 (1941).
[3] D. L. Lambert and R. Beer, Astrophys. J. **177**, 541 (1972).
[4] J. M. Lents, J. Quant. Spectrosc. Radiat. Transf. **13**, 297 (1973).
[5] R. A. Fifer, *Fundamentals of Solid Propellant Combustion*, edited by K. K. Kuo and M. Summerfield (American Institute of Aeronautics and Astronautics, New York,1984).
[6] P. E. Cade and W. M. Huo, J. Chem. Phys. **47**, 614 (1967).
[7] S. V. O'Neil and H. F. Schaefer III, J. Chem. Phys. **55**, 394 (1971).
[8] W. Meyer and P. Rosmus, J. Chem. Phys. **63**, 2356 (1975).
[9] P. C. Engelking and W. C. Lineberger, J. Chem. Phys. **65**, 4323 (1976).
[10] P. J. Hay and Thom H. Dunning Jr., J. Chem. Phys. **64**, 5077 (1976).
[11] P. Rosmus and W. Meyer, J. Chem. Phys. **66**, 13 (1977).
[12] P. Rosmus and W. Meyer, J. Chem. Phys. **69**, 2745 (1978).
[13] P. F. Zittel and W. C. Lineberger, J. Chem. Phys. **65**, 1236 (1976).
[14] D. Cvejanovic, A. Adams, and G. C. King, J. Phys. B **11**, 1653 (1978).
[15] G. Frenking and W. Koch, J. Chem. Phys. **84**, 3224 (1986).
[16] K. N. Joshipura, M. Vinodkumar, and U. M. Patel, J. Phys. B **34**, 509 (2001).
[17] Rajendra Pd. and P. Chandra, J. Chem. Phys. **114**, 7450 (2001).
[18] E. M. Goldfield and K. P. Kirby, J. Chem. Phys. **87**, 3986 (1987).
[19] L. A. Morgan, C. J. Gillan, J. Tennyson, and X. Chen, J. Phys. B **30**, 4087 (1997).
[20] L. A. Morgan, J. Tennyson, and C. J. Gillan, Comput. Phys. Commun. **114**, 120 (1998).
[21] J. Tennyson, J. Phys. B **29**, 1817 (1996).
[22] Y. K. Kim and M. E. Rudd, Phys. Rev. A **50**, 3954 (1994).
[23] W. Hwang, Y. K. Kim, and M. E. Rudd, J. Chem. Phys. **104**, 2956 (1996).
[24] J. S. Rajvanshi and K. L. Baluja, Phys. Rev. A **81**, 022709 (2010).
[25] C. J. Noble and P. G. Burke, J. Phys. B **19**, L35 (1986).
[26] P. G. Burke and K. A. Berrington, *Atomic and Molecular Processes: An R-Matrix Approach* (Institute of Physics Publishing, Bristol, 1993).
[27] C. J. Gillan, J. Tennyson, and P. G. Burke, *Computational Methods for Electron-Molecule Collisions*, edited by W. M. Huo and F. A. Gianturco (Plenum, New York, 1995).
[28] K. L. Baluja, P. G. Burke, and L. A. Morgan, Comput. Phys. Commun. **27**, 299 (1982).
[29] L. A. Morgan, Comput. Phys. Commun. **31**, 419 (1984).
[30] B. M. Nestmann, K. Pfingst, and S. D. Peyerimhoff, J. Phys. B **27**, 2297 (1994).
[31] J. Tennyson, J. Phys. B **29**, 6185 (1996).
[32] A. Faure, J. D. Gorfinkiel, L. A. Morgan, and J. Tennyson, Comput. Phys. Commun. **144**, 224 (2002).
[33] T. H. Dunning and P. J. Hay, *Methods of Electronic Structure Theory*, edited by H. F. Schaefer (Plenum, New York, 1977), Vol. 2.
[34] S. Kaur, K. L. Baluja, and J. Tennyson, Phys. Rev. A **77**, 032718 (2008).
[35] E. S. Chang and A. Temkin, Phys. Rev. Lett. **23**, 399 (1969).
[36] F. A. Gainturco and A. Jain, Phys. Rep. **143**, 347 (1986).
[37] N. Sanna and F. A. Gianturco, Comput. Phys. Commun. **114**, 142 (1998).
[38] Y. Itikawa, Phys. Fluids **16**, 831 (1973).
[39] I. P. Shkarofsky, Can. J. Phys. **39**, 1619 (1961).